Spectroscopic studies of the $Ar(H_2)_2$ compound crystal at high pressure and low temperatures

Lorenzo Ulivi*
Istituto di Elettronica Quantistica, Consiglio Nazionale delle Ricerche, via Panciatichi 56/30, I-50127 Firenze, Italy

Roberto Bini
Dipartimento di Chimica, Università di Firenze, Via G. Capponi 9, I-50121 Firenze, Italy
and LENS, European Laboratory for Non-linear Spectroscopy, Largo Enrico Fermi 2, 50125 Firenze, Italy

Paul Loubeyre
Laboratoire Etats Extrêmes Statiques, DIF/DPTA/SPMC, CEA 91680 Bruyeres-Le-Chatel, France

René LeToullec
Physique des Milieux Condensés, Université Pierre et Marie Curie, Paris VI, 4 place Jussieu, 75252 Paris 05, France

H. J. Jodl
Universität Kaiserslautern, Fachbereich Physik, Erwin-Schrödinger-Strasse, D-67663 Kaiserslautern, Germany
and LENS, European Laboratory for Non-linear Spectroscopy, Largo Enrico Fermi 2, 50125 Firenze, Italy
(Received 9 February 1999)

Fourier-transform infrared and Raman studies are performed on $Ar(H_2)_2$ compound single crystals over a large pressure (5–30 GPa) and temperature (30–300 K) range in a diamond-anvil cell. The effect of polarization on the infrared absorption is investigated. On the basis of the spectroscopic features and comparing to the cases of pure solid H_2 and of matrix isolated H_2 in argon crystal, we assign the quite complex infrared spectra to the pure vibron and vibron plus phonons and vibron plus rotons combination bands. The difference of the infrared and Raman vibron frequency, as a function of pressure, is interpreted quantitatively with reference to vibrational coupling between hydrogen molecules, as in the hydrogen crystal case. Information on the structural properties can thus be derived. Finally, this study highlights the similarity in the molecular problems for the $Ar(H_2)_2$ compound and for solid hydrogen. [S0163-1829(99)12529-3]

I. INTRODUCTION

The study of molecular crystals has undergone renewed interest in recent years, with the possibility of performing accurate and detailed experiments under static pressures up in the megabar range. Important properties such as the insulator-metal phase transition, the phase diagram of binary mixtures, or the quantum effects of density could be investigated. Among the molecular crystals, solid hydrogen keeps a particular status for its quantum nature and its fundamental interest. Many spectroscopic investigations have been performed on solid hydrogen at high pressure. One of the issues discussed most frequently refers to the pressure induced insulator-metal transition related to the softening of the vibron as an indication of the weakening of the intramolecular bond and possible structural phase transitions.[1]

A completely new phenomenology has emerged with the unexpected discovery that the application of high pressure to binary mixtures may stabilize ordered solid phases of two molecular systems mixed in stoichiometric proportions.[2–5] These are, under all aspects, new compounds where the molecules are held together by weak van der Waals forces. After the first identification of the $He(N_2)_{11}$ compound, others have been found such as $Ne(He)_2$, $Ar(H_2)_2$, $CH_4(H_2)$, etc. The importance of these systems lays in the fact that they are useful to study interactions among simple molecules in a different environment. Different structures than those in the pure molecular solid are stabilized. Furthermore, these make it possible to create two-dimensional layers of interacting molecules.

Interestingly, the $Ar(H_2)_2$ compound has been proposed as a suitable system for observing extreme effects originally predicted to take place in pure hydrogen, namely, the pressure-induced insulator-metal transition.[6] The experimental situation in the 200 GPa range is confusing since a possible metallization has been reported in Raman measurements[5] whereas no signs of the disappearance of the vibron nor Drude edge due to free electrons have been observed in IR measurements to 240 GPa.[7] It is suspected that the orientation of the crystal to the load axis might strongly influence the properties of the system at extreme pressures. Also, the analogy with the hydrogen problem has been questioned under the argument of the possible hybridization of the Ar orbitals with those of the H_2 molecules.

We show below that, at least to the 50 GPa range, there are strong analogies between the spectral data of $Ar(H_2)_2$ and solid H_2. The same well-known excitations of solid H_2 are here observed in a different environment. The structural properties of this compound, discussed extensively in the next paragraph, create in the sites occupied by the hydrogen molecules a crystal field with a different symmetry than that in the hcp pure hydrogen crystal. This configuration can have intriguing consequences on some physical properties, such as the rotation of the molecules and the H_2-H_2 coupling. Prin-

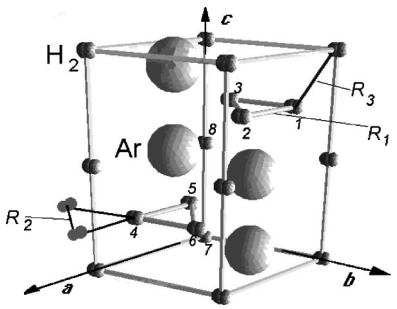

FIG. 1. Drawing of the unit cell of the $Ar(H_2)_2$ compound. The H_2 molecules are shown as little dumbbells, and the Ar atoms as large spheres. The c axis is vertical and the origin is coincident with molecule No. 7. The distances R_1, R_2, and R_3, used in Sec. V, are indicated.

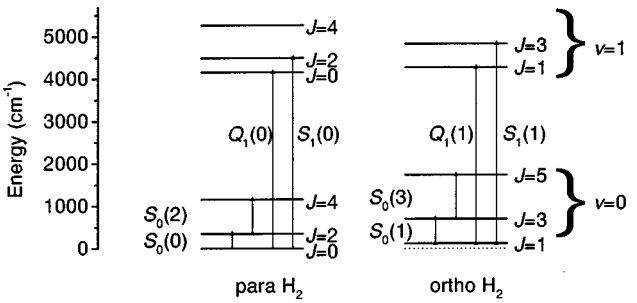

FIG. 2. Rotational and vibrational energy level diagram of the hydrogen molecule including the standard nomenclature of molecular transitions.

cipally the latter aspect will be investigated quantitatively to interpret the spectroscopic data. In addition, our set of experimental data of vibron frequencies versus pressure, obtained at low pressure, is an important prerequisite for the analysis of the synchrotron infrared absorption data obtained at ultrahigh pressure (up to 220 GPa).[7]

In the next section we discuss in some detail the structure of the $Ar(H_2)_2$ compound, on the basis of the available x-ray data.[5] Section III is a brief description of the experimental setup, while in Sec. IV the spectroscopic results are presented and the observed spectral components assigned. In Sec. V we discuss in detail two aspects of the data. One is the splitting of the IR vibron observed at low temperature. The second part of this section is devoted to the calculation of the difference between the Raman and the IR vibron modes, and the comparison with the experiment.

II. STRUCTURE OF $Ar(H_2)_2$

When a 2:1 mixture of H_2 and Ar gases is pressurized in a diamond-anvil cell at room temperature, it solidifies at about 4.3 GPa into an homogeneous solid. If pressure rises smoothly, in some cases, visual observation suffices to identify a faceted crystal in the cell, in equilibrium with the fluid mixture. The structure of this compound has been determined by synchrotron x-ray diffraction.[5] The diffraction results are consistent with theoretical considerations by Gibbs free energy calculations, which predict a stable structure isomorphous to the $MgZn_2$ Laves phase. The unit cell is hexagonal, and contains eight H_2 molecules and four Ar atoms. Dimensions of the unit cell at 6.2 GPa are $a=5.211(2)$ Å and $c=8.482(7)$ Å.[5] The crystal structure of the $MgZn_2$ alloy was determined first by x-ray analysis and density measurements by Friauf.[8] Accordingly, he specified the position of Zn and Mg atoms and proposed the two space groups D_6^6 $(P6_322)$ or D_{6h}^4 $(P6_3/mmc)$. More recent results have confirmed that the space group is D_{6h}^4.[9,10] The unit cell of the $Ar(H_2)_2$ compound is drawn in Fig. 1, where the small dumb bells represent the hydrogen molecules and the larger circles are Ar atoms. Two molecules of a neighboring cell are also shown. The H_2 molecules are numbered from 1 to 8 and the distances R_1, R_2, and R_3 are here indicated for future reference.

The four Ar atoms occupy equivalent sites of symmetry C_{3v}, at the coordinates $(xyz)=(1/3,2/3,v)$, $(1/3,2/3,1/2-v)$, $(2/3,1/3,1/2+v)$, $(2/3,1/3,\bar{v})$ while the H_2 molecules are positioned in two sites of different symmetry, namely, two molecules (7 and 8 in Fig. 1) at the positions (0, 0, 0), (0, 0, 1/2), in sites of symmetry D_{3d}, and six molecules (labeled from 1 to 6 in Fig. 1) at the positions $(\bar{u},u,3/4)$, $(2u,u,3/4)$, $(\bar{u},2\bar{u},3/4)$, $(u,\bar{u},1/4)$, $(2\bar{u},\bar{u},1/4)$, $(u,2u,1/4)$, in sites of symmetry C_{2v}. Molecules 7 and 8 are vertex of tetrahedra, whose bases are formed by molecule 6 of the same cell and molecules 4 and 5 of adjacent cells. The parameters u $(1/2<u<1)$ and v $(0<v<1/2)$ have not been determined by x-ray measurements. In particular, depending on the value of u (see Ref. 8), the equilateral triangles depicted in Fig. 1 change their dimensions. For $u=5/6$ all the molecules on the $z=1/4$ and $z=3/4$ planes are arranged on equal equilateral triangles, at a distance $R_1=R_2=a/2$. If $c=\sqrt{8/3}\times a$ then we have also $R_3=a/2$.

As it will be demonstrated in this study, similarly to what happens in pure solid hydrogen, the H_2 molecule in this compound crystal at relatively low pressure can perform almost free rotations and vibrations, whose energy levels are only slightly displaced from that of the free molecules. Also the distinction between para and ortho hydrogen[11] is still valid in this solid. For clarity on the nomenclature, therefore, we report in Fig. 2 a scheme of the first few rotovibrational levels of the ortho and para species of the hydrogen molecule. Among the transitions represented in the figure, the pure rotations $S_0(0)$, $S_0(1)$, $S_0(2)$, and $S_0(3)$, and the vibrations $Q_1(0)$ and $Q_1(1)$ are observed in the Raman spectra, while the IR spectra are characterized, in the frequency region investigated, by features due to vibrational and rotovibrational transitions (see Sec. IV).

III. EXPERIMENT

The Ar gas (purity 5.0) and H_2 gas (purity 4.5) were premixed in the ratio 1:2 in a bottle, and left to equilibrate for a few days. Subsequently the sample was filled into the membrane diamond-anvil cell (MDAC) (Ref. 12) via a high pressure gas loading system. Solidification, obtained rising smoothly the pressure above 4.3 GPa at room temperature, produced usually a faceted oriented hexagonal crystal.

The Raman spectra, excited by an Ar-ion laser either in forward scattering or at an angle, were collected by a Spex triple-mate spectrometer equipped with a cooled CCD detector, in the range of the H_2 rotation lines (350−

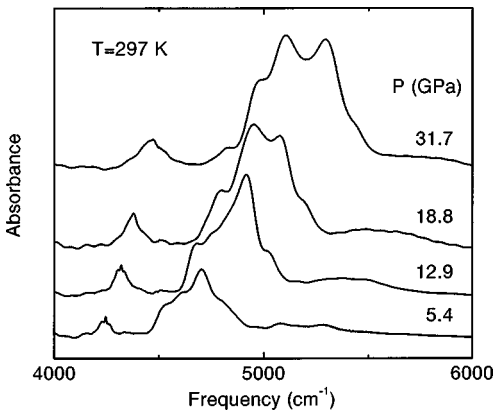

FIG. 3. Overview of the pressure evolution of the FTIR spectrum at room temperature. Vibron excitations contribute to the absorption feature centered (at 5.4 GPa) around 4250 cm^{-1} (referred to in the text as the *vibron band*), while the band between 4450 and 4900 cm^{-1} is due to vibron-rotons and vibron-phonons combinations.

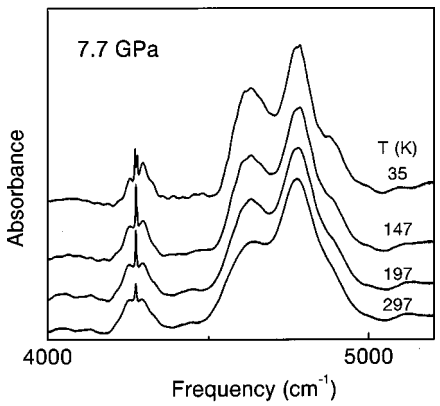

FIG. 4. Infrared spectra as a function of temperatures at a constant pressure of 7.7 GPa. Decreasing temperature, the vibron band shows more clearly its structure, as discussed in the text.

-1000 cm^{-1}) and in the region of the H_2 vibron ($\simeq 4200$ cm^{-1}) with a typical resolution of 2–3 cm^{-1}. The infrared spectra have been recorded with a FTIR-spectrometer (Bruker 120 HR) equipped with a InSb detector in the region of 4000–6000 cm^{-1}, with a typical resolution of 0.5 cm^{-1}. The infrared beam was focused on the sample in the MDAC via Cassegrain optics. This system allows a remote control and measurement of the sample pressure (by means of *in situ* observation of the ruby fluorescence[13]) and the sample temperature, independently, without altering the alignment of the MDAC, which is thermally coupled to a closed-cycle cryostat. This complete system, for the measurements of IR spectra at high pressure and low temperature, has been described in detail elsewhere.[14,15]

Many samples have been used for these measurements. By finely tuning pressure, while observing visually the sample, we were able to grow perfect, faceted single crystals of the $Ar(H_2)_2$ compound with a fluid mixture of equal concentration surrounding it. The faceted crystal has been obtained either with the *c* axis almost perpendicular and parallel to the faces of the diamonds. Using a polarizer, it was therefore possible to obtain spectra with radiation polarized in two nonequivalent directions, namely, parallel or perpendicular to the *c* axis, as described in the following.

IV. RESULTS

A. Description of spectra

An overview of the absorbance spectra at room temperature and different pressures is displayed in Fig. 3. The consideration of the frequency ranges where absorption bands appears, in combination with the knowledge of molecular excitations in the hydrogen solid suggests a rough assignment. The band located in the range 4200–4500 cm^{-1} is to be assigned to excitations closely related to the intramolecular vibration, and will be referred to in the following as the vibron band. This band is structured, and shows particular polarization characteristics. The origin of this structure and the assignment of its components is discussed in the following subsection. Raising the pressure, the frequency of this band increases almost linearly in energy, and its intensity grows considerably.

A stronger band, containing a few broad maxima, whose relative intensities vary drastically with increasing pressure, is evident in the range 4500–5000 cm^{-1}. The decomposition of this complex pattern, discussed later in detail, shows that the frequencies of the band maxima evolve quite differently with pressure. With respect to the fundamental mode the frequency of this band is shifted, roughly, by the energy corresponding to the rotational excitations $J=0\rightarrow 2$ or $J=1\rightarrow 3$ of the H_2 molecule. Therefore, at least two of the IR peaks observed in this frequency region are due to excitations that correspond to a combination of one vibration and one rotation jump of the H_2 molecule. The total intensity of this band in comparison to the one in the former region is about ten times larger at each pressure.

Two further broad bands are present in the region 5000–6000 cm^{-1} that may be associated to the combination of one vibron plus a higher rotational transition. These bands are pretty weak in comparison to all other described features, and merge into one broad excitation increasing pressure.

In cooling the sample at moderate pressure we hoped to observe more detailed spectra (see Fig. 4, spectra taken between 300 and 30 K). However, the width of the various bands does not change too much, and the whole pattern is pretty much the same at different temperatures, aside from two significant changes. In the first region (4100–4500 cm^{-1}) the zero phonon line splits into a sharp doublet on cooling. In the second range (4500–5000 cm^{-1}) only the first broad band around 4600 cm^{-1} increases remarkably in intensity on cooling; due to the rough assignment above this might be a combination mode of a H_2 vibron and a rotation of the para modification of H_2.

To complement infrared spectra we performed also Raman scattering on the $Ar(H_2)_2$ compound crystal. In Fig. 5 we present some Raman spectra, at room temperature and different pressures, in the region of the rotational excitations, which contain four well resolved bands between 300–1200 cm^{-1}, and in the region of the vibron, where we observe one single band near 4200 cm^{-1}.

The assignment of the rotational part of Raman spectra is straightforward. The four bands, from lower to high fre-

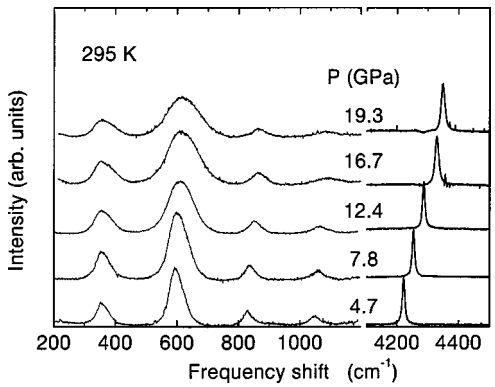

FIG. 5. Pressure dependence of the rotational and vibrational Raman spectrum of the $Ar(H_2)_2$ compound crystal at room temperature. The four pure rotational lines $S_0(J)$, $J=0\cdots3$ are clearly observed at frequencies similar to those of the single molecule, in the low frequency region. The frequency of the intense vibron peak, observed above 4200 cm^{-1}, increases rapidly with pressure.

quency shift, are identified as $S_0(0)$, $S_0(1)$, $S_0(2)$, and $S_0(3)$ (see Fig. 2 for the nomenclature). The presence of well resolved rotational lines demonstrates that the H_2 molecules are freely rotating in this compound as in the pure H_2 crystal.

The relative integrated intensity of these four bands is almost constant in pressure. With respect to $S_0(1)$, the intensities of $S_0(0)$, $S_0(2)$, and $S_0(3)$ have the average values 0.29, 0.12, and 0.09, respectively. These may be compared to the theoretical values 0.34, 0.15, and 0.10 which are calculated for one isolated molecule.

The single band in the Raman vibrational spectrum (Fig. 5) corresponds to both single molecules transitions $Q_1(0)$ and $Q_1(1)$, that, as in pure solid H_2 at high pressure, are not resolved. Up to a pressure of about 20–25 GPa, all the rotational lines are well resolved and nonoverlapping. We can measure then the frequency shift of the modes with pressure and the broadening of bands.

B. Analysis of spectra and mode assignment

We discuss in this section the assignment of the infrared vibron band. This band, as mentioned in the Introduction, is structured, and its shape changes drastically with temperature, as appears from Fig. 6(a). When our sample consisted of a single crystal having the *c* axis parallel to the two diamond faces it has been possible to obtain infrared spectra with incident radiation polarized in two nonequivalent directions. These polarized spectra, obtained for a crystal of known orientation, have been of fundamental help for the assignment of the observed bands to different crystal modes.

A series of 24 spectra at 12 different pressures from 7.7 to 36 GPa has been measured, at room temperature, using two different polarizations of the incident radiation at each pressure. The shape of the rotovibrational combination bands, located above 4500 cm^{-1}, does not show any significant difference when the spectra collected with different polarizations are compared, demonstrating that this band is essentially depolarized. Very evident differences, on the other hand, are manifest in the region of the vibron peak [Fig. 6(b)] where the narrow central peak and two sidebands dis-

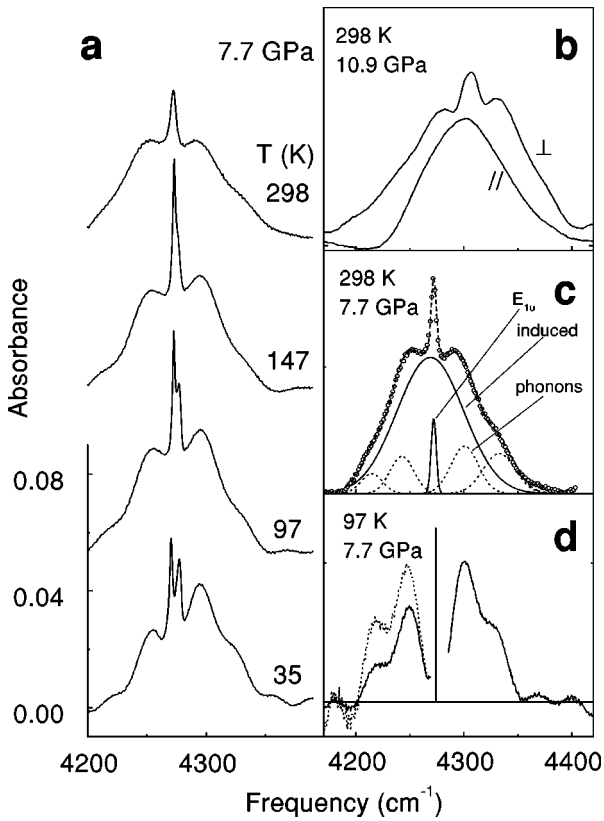

FIG. 6. Infrared vibron band: (a) evolution with temperature; (b) spectra obtained with polarization either parallel (∥) or perpendicular (⊥) to the direction of the *c* axis of the crystal; (c) decomposition of the band as it results from the discussion in the text; (d) experimental phonon branches (Stokes and anti-Stokes side, solid line) obtained by subtraction of the E_{1u} and induced bands from the experimental spectrum. The dotted line is the anti-Stokes branch multiplied by the Boltzmann factor.

appear completely with light polarized parallel to the *c* axis of the crystal. This demonstrates the different origin of the broader unpolarized band from that of the narrower peaks.

Since the selection of the polarization has been done without altering any other aspect of the experimental setup, it is possible to obtain very good results by a simple subtraction of the spectra measured in the two polarizations. This procedure puts in evidence three bands, which then appears in the difference spectra on a zero background. The central peak has a width of about 7 cm^{-1} at room temperature, and is superimposed to two broader bands, symmetrically displaced at the sides, but with a different intensity.

Since the structure of the $Ar(H_2)_2$ compound is known, we can analyze the activity of the vibron mode, and its polarization properties, on the basis of group theory arguments. In Table I the correlation diagram of the hydrogen vibron mode is shown, according to the proposed D_{6h}^4 structure.

In the D_{6h}^4 structure the fundamental vibrational Σ_g^+ mode of the isolated H_2 molecule splits into four components for the H_2 molecules in sites C_{2v} and into two components for the two molecules in sites D_{3d}. The optical activity is restricted to two Raman and one infrared bands (A_{1g}, E_{2g}, and E_{1u}, respectively) for the molecules in sites C_{2v}, and to only one Raman band (A_{1g}) for the molecules in sites D_{3d}. The two total symmetric modes will be distinguished in the

TABLE I. Correlation diagram for the hydrogen vibron mode in the $Ar(H_2)_2$ compound crystal.

Molecular symmetry $D_{\infty h}$	Site symmetry	Factor group symmetry D_{6h}	Activity
		A_{1g}	Raman
Σ_g^+	(C_{2v}) A_1	E_{2g}	Raman
		B_{1u}	inactive
		E_{1u}	infrared
Σ_g^+	(D_{3d}) A_{1g}	A_{1g}	Raman
		B_{2g}	inactive

following with the notation A'_{1g} and A''_{1g}. The analysis by means of group theory shows also which are the polarization properties of the IR active vibron. It results that for the E_{1u} infrared mode, the electric vector is oscillating in the ab plane.

The simplicity of the measured vibrational Raman spectrum (Fig. 5) contrasts with the expected number of active components. A justification why some of the Raman frequencies are not observed will be given in the following.

The observed infrared spectrum can now be analyzed on the basis of these results. The depolarized spectra have been collected with the crystal c axis coincident with the optical path, therefore E_{1u} should be observable, since the electric vector is oscillating in the ab plane. In the polarized spectra, collected with the c crystal axis perpendicular to the optical path, the IR active mode should be observed only when the polarization is perpendicular to the c axis. Therefore, one of the three narrow components (actually, the central one, as it will be clear in the following), that is superimposed to the broad band, and disappears when the polarization is rotated [see Fig. 6(b)] should be assigned to the allowed E_{1u} infrared vibron. The presence of the unpolarized broad band and of the two other narrow bands remains to be discussed.

It is illuminating at this point to repeat the group theory analysis for pure hydrogen in the hcp phase. The space group is the same of the $Ar(H_2)_2$ compound D_{6h}^4 $(P6_3/mmc)$ but all molecules are sitting on equivalent sites of symmetry D_{3h} $(\bar{6}m2)$. The result is that no IR active vibron mode is predicted in this structure. The Q branch of the IR absorption spectrum of pure solid H_2, however, has been known for a long time, from the measurements of Gush[16] at low pressure, those of Jean-Louis at low temperature and higher pressure,[17–19] to the more recent ones, at room temperature, in the megabar pressure range.[20] This band is asymmetric, and has a width of about 13 cm^{-1} at low pressure and low temperature,[16] growing to about 180 cm^{-1} at 80 GPa and room temperature.[20] The IR vibron band in H_2 is interpreted as induced by the presence of ortho-H_2 molecules in the crystal.[16] Since these molecules are randomly distributed among the lattice sites, no cancellation effect due to the symmetry of the crystal occurs in this case. A more rigorous analysis[21] leads to the conclusion that this band is essentially due to double transitions, in which a purely vibrational transition in one molecule is accompanied by an orientational transition in one or more of its nearest neighbor ortho molecules. The stronger induction mechanism is due to the permanent quadrupole of the H_2 molecule, that, however, has a zero expectation value for a para-H_2 molecule in the $J=0$ state.

In $Ar(H_2)_2$ the situation is more complicated than in pure hydrogen. Since the H_2 molecule does not possess a permanent dipole moment, also in this case the IR activity is due to dipoles induced by neighboring molecules. However, here, group theory analysis predicts, even for a perfectly ordered crystal, the possibility of a symmetry allowed vibron mode, with dipole moment oscillating in the ab plane. Experimentally, in fact, not a single band but a structured feature is observed in the vibron region, that results then as the sum of six components [see Fig. 6(c)], whose assignment is now clear. The polarized central peak is E_{1u} zero phonon IR active vibron mode, associated to the six H_2 molecules per unit cell in the C_{2v} sites. This will be denoted in the following, analogously to the pure H_2 case[17] as Q_q, and corresponds to the $Q_1(J)$ excitation of the single molecule. At room temperature and high pressure, the $Q_1(0)$ and $Q_1(1)$ lines are not resolved. The other two pairs of polarized bands, symmetrically displaced with respect to the E_{1u} peak, are to be attributed to the Stokes (higher frequency) and anti-Stokes (lower frequency) components of combination of vibration and phonons. The existence of these low frequency excitations is a characteristic of this compound that has no reciprocity in pure H_2. This assignment is confirmed by the spectra obtained at low temperature, as it will be described in detail in the following.

The unpolarized broad band has a width which increases with pressure from about 40 cm^{-1} at $p=5$ GPa to about 120 cm^{-1} at 30 GPa. We assign this band to the vibration of all the H_2 molecules (i.e., those on both C_{2v} and D_{3d} sites) in which the dipole moment is induced by neighboring ortho molecules by means of multipole induction or overlap mechanism. The ortho molecules are randomly distributed in the lattice sites, therefore this contribution cannot be canceled out by the symmetry of the crystal. This is exactly what happens in pure H_2, and this band corresponds, in our interpretation to the one observed in H_2 in all different experimental conditions.[16,17,20] The width of this band in pure H_2, as measured, for example, by Gush, is narrower, but this can be easily explained by the lower pressure and temperature of the sample in that case. From Fig. 1 of Ref. 20 one can derive for this width in H_2 the value of about 180 cm^{-1} at room temperature and 80 GPa. Since we measured this broad band between 5 and 30 GPa, we can extrapolate to zero pressure, and we reach a value of about 12 cm^{-1}, pretty

close to the bandwidth by Gush.[16] Since the dipoles induced on the molecules are randomly oriented, this band is not polarized.

All the spectra, recorded as a function both of temperature and of pressure have been fitted on the basis of this assignment. A typical decomposition of spectrum into individual bands is presented in Fig. 6(c). The best fit of the phonon side bands is obtained with two components both on the Stokes and on the anti-Stokes side.

It is noteworthy to observe the behavior of this band lowering temperature. The change of intensity of the Stokes phonon band with respect to the anti-Stokes is dramatic. This is documented in Fig. 6(a), showing the temperature evolution of the vibron band, and in Fig. 6(d), where we show the phonon bands, obtained subtracting from the experimental spectrum at $T=97$ K the allowed (E_{1u}) and induced vibron band, derived from the fit of the whole band.

The intensity of the anti-Stokes side, once multiplied for the population factor $\exp\{-h(\nu-\nu_0)/kT\}$ [dashed line in Fig. 6(d)], where ν_0 is the frequency of the E_{1u} vibron mode and k is the Boltzmann constant, is perfectly comparable to that measured on the Stokes side. This nicely confirms the assignment of these bands as due to combinations with phonons. The profile of this structure can be considered representative of the density of states of low frequency phonon. These low energy excitations are induced by the presence of the heavy Ar atoms in this compound. In fact, considering the typical values of the phonon energies in pure Ar (see, for example, Ref. 22) one obtains, for solid Ar at 10 K, values between 0 and 100 cm^{-1}, which compare perfectly with the spectrum of Fig. 6(d). This indicates, therefore, that the phonon modes which involve the Ar atoms are essentially uncoupled from those that involve the lighter H_2 molecules. This will be more evident after the analysis of the H_2 phonon modes, discussed in the following.

We now discuss the pressure shift of the modes that contribute to the 4200–4500 cm^{-1} band. The IR allowed vibron frequency has been derived from the experimental runs done with polarized radiation since in these cases the subtraction of the spectra polarized in the two independent directions gives, even at the highest pressure, a very evident narrow peak. In these cases the c axis of the crystal is perpendicular to the load axis of the cell. A significative difference in the IR peak frequency is measured if one considers instead the maximum of the broad band observed when the crystal c axis is oriented parallel to the load axis, and no polarization analysis is possible. In these cases the IR frequency results higher, of a quantity of the order of 30 cm^{-1} at 30 GPa. This indicates a strong elastic anisotropy of this compound. For all the subsequent analyses we have used the data obtained with the c axis perpendicular to the load axis of the cell. The measured pressure shift of the IR and Raman vibron of $Ar(H_2)_2$ are reported in Fig. 7, as a function of pressure, where they are compared with analogous quantities measured for pure H_2 (from the smoothed values of Ref. 23, reported as a function of pressure by means of the H_2 equation of state[24,25]). As in pure H_2 the IR vibron peak is at a higher frequency than the corresponding Raman one, and the difference amounts to about 70 cm^{-1} at 30 GPa. This difference for the $Ar(H_2)_2$ compound will be quantitatively analyzed in the next section.

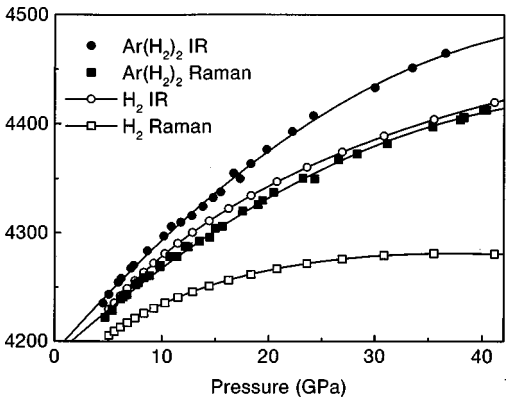

FIG. 7. Pressure shift of the IR and of the Raman vibron modes in $Ar(H_2)_2$ (solid symbols fitted with second order polynomials) compared with analogous data obtained for H_2 (empty symbols, joined by splines). The fit parameters are given in Table II.

Before discussing the region of the IR spectrum in the range 4500–5500 cm^{-1}, it is useful to analyze the pure rotational Raman spectrum recorded at room temperature in the range 200–1200 cm^{-1} (see Fig. 5). The pressure dependence of the frequencies of the four band maxima is displayed in Fig. 8. The frequencies of the bands are fitted linearly, and the resulting parameters are collected in Table II. Our room temperature data of the compound crystal are very close, within error, to our own room temperature data and low temperature values of natural solid H_2 (see Table II). First, therefore our assumption of freely rotating H_2 molecules in $Ar(H_2)_2$ as in solid H_2 is justified. The second

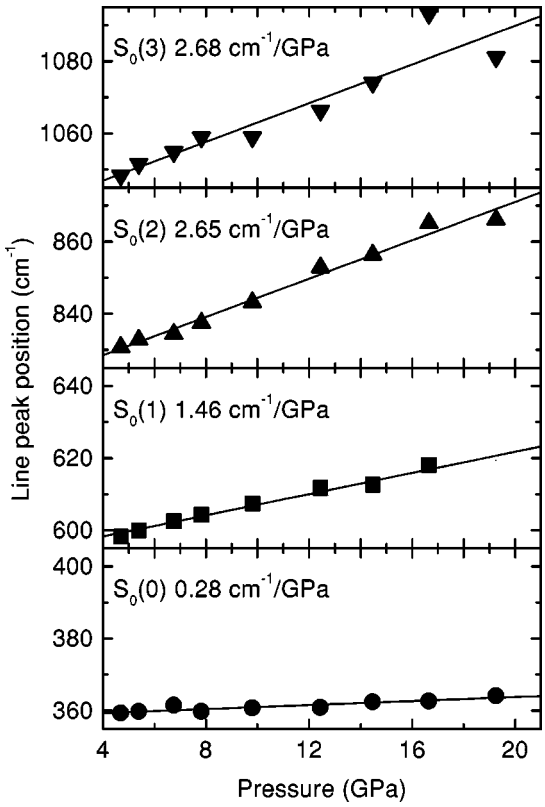

FIG. 8. Pressure shift of the pure rotational Raman lines in $Ar(H_2)_2$. Numerical values for the slopes are reported in each figure.

TABLE II. Pressure dependence of frequencies of Raman and infrared excitations in the $Ar(H_2)_2$ compound crystal, compared to pure and matrix isolated H_2. The coefficients Ω_2 and Ω_3 of a polynomial fit $\omega(p)=\omega_0+\Omega_1 p+\Omega_2 p^2+\Omega_3 p^3$ are sometimes indicated in brackets below Ω_1, if necessary.

	$Ar(H_2)_2$ (300 K)		H_2		H_2 in Ar	
	ω_0 cm^{-1}	Ω_1 cm^{-1}/GPa	ω_0 cm^{-1}	Ω_1 cm^{-1}/GPa	ω_0 cm^{-1}	Ω_1 cm^{-1}/GPa
Rotons (Raman)						
$S_0(0)$	358	0.28	361	0.01	351[a]	
$S_0(1)$	592	1.46	595	1.58	584[a]	
$S_0(2)$	818	2.65	816	3.69		
$S_0(3)$	1036	2.68	1036	2.98		
Vibron (Raman)						
$Q_1(J)$	4185.8	9.027	4166[f]	8.9[f]		
		(−0.08539)		(−0.21)[f]		
$Q_1(1)$					4153[b]	9.42232[b]
						(−0.1636)[b]
						[0.00179][b]
Vibron (infrared)						
$Q_1(J)$	4189.4	11.472			4142 [e]	
		(−0.10857)				
$Q_1(0)$			4153[c]	26[c]		
$Q_1(1)$			4146[c]	25[c]		
			4166[f]	14[f]		
				(−0.28)[f]		
vibron+phonons (IR)						
$Q_{r'}$	4202	11.50			4257[e]	
Q_r	4198	14.64			4165[e]	
Q_p	4184	6.46			4229[e]	
$Q_{p'}$	4182	9.23			4037[e]	
vibron + rotons (IR)						
$S_1(0)$ and $Q_1(J)+S_0(0)$	4516	13.27	4500[c]	25[c]	4478[e]	
		(−0.13)				
$S_1(1)$ and $Q_1(J)+S_0(1)$	4700	17.39	4732[c]	41[c]	4691[e]	
		(−0.16)				
			4760[d]	9.5[d]		
				(−0.083)[d]		
vibron + phonons (IR)						
Q_{R1}	4379	26.30				
		(−0.25)				
Q_{R2}	4448	28.44				
		(−0.23)				
Q_{R3}	4479	41.99				
		(−0.52)				
Q_{R4}	4583	40.77				
		(−0.42)				
Q_R			4220[c]	190[c]		
			4641[d]	31.37[d]		
				(−0.25)[d]		

[a] $T=13$ K, Ref. 30.
[b] $T=295$ K Ref. 31.
[c] Results of a linear fit up to 1 GPa, of the data of Ref. 19 (4.2 K).
[d] Results of a parabolic fit in the range 12–40 GPa, of the data of Ref. 1 (295 K).
[e] Ref. 32.
[f] Results of a parabolic fit to the low pressure part of the model of Ref. 23 (295 K).

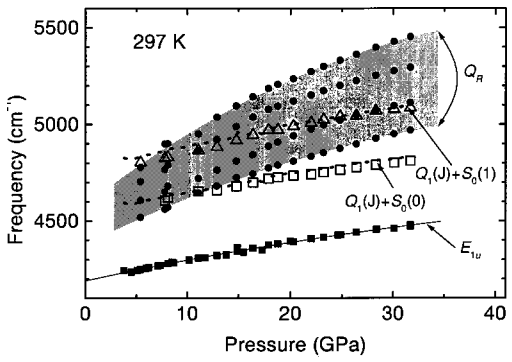

FIG. 9. Pressure dependence of the E_{1u} IR vibron (solid squares fitted by a polynomial) and of vibron-phonon combination mode frequencies (solid dots). The bands whose frequencies are indicated by empty symbols are assigned to vibron roton combination bands [squares: $S_1(0)$ and $Q_1(J)+S_0(0)$, triangles: $S_1(1)$ and $Q_1(J)+S_0(1)$]. The dotted lines correspond to the sum of the measured Raman $S_0(0)$ and $S_0(1)$ frequencies to the infrared E_{1u} vibron frequency.

result is the fact that the slopes Ω_1 increase with increasing rotational quantum number. This happens also in solid pure H_2,[26] and is not surprising, since for higher J values, the internuclear distance is larger, due to centrifugal stretching, and the molecule is more perturbed by the interaction with neighboring molecules. The pressure slope of the mode frequency is about 4 times larger for the vibron than for the rotations.

Now we will analyze the region 4500–5000 cm^{-1} of the IR spectrum, which we already roughly assigned to a vibron plus rotations of the H_2 molecule in the $Ar(H_2)_2$ compound crystal. After a careful analysis of all ($\simeq 100$) spectra taken at different pressures (5–30 GPa) and temperatures (30–300 K), a consistent pattern of evolution with pressure of band frequencies, widths and intensities could be established. In Fig. 9 the band positions are reported as a function of pressure. The dotted lines are obtained by summing the measured Raman $S_0(0)$ and $S_0(1)$ frequencies to the one of the E_{1u} infrared allowed vibron line. Therefore the assignment of the two sets of frequencies, which evolve rather flat with pressure, to the vibron plus rotations combination bands is evident. These bands are represented by empty squares [$S_1(0)$ and $Q_1(J)+S_0(0)$] and empty triangles [$S_1(1)$ and $Q_1(J)+S_0(1)$] in Fig. 9. Then, we attribute the four band, whose frequencies evolve more steeply with pressure (solid dots in Fig. 9), to the vibron plus high frequency phonons ($Q_{R1}\cdots Q_{R4}$). These bands represent essentially an unique density of states of high frequency phonons, that couple to a H_2 vibron. Therefore, in Fig. 9, we shaded the corresponding frequency region. In Table II the parameters describing the pressure evolution of these bands are collected, and compared to the data of pure solid H_2 and of matrix isolated H_2 in solid argon.

The dispersion of the high frequency phonon sideband in $Ar(H_2)_2$ at $p \simeq 15$ GPa is about 300 cm^{-1} and at $p \simeq 30$ GPa it reaches 600 cm^{-1}. Extrapolation of this width to $p=0$ achieves $\simeq 100$ cm^{-1}. This value might be compared to the density of states of solid H_2 which is about 100 cm^{-1} at ambient pressure (see, e.g., Ref. 27). The evolution of phonon bands with pressure in solid H_2 is similar to the one measured here. The E_{2g} phonon, measured directly by Raman spectroscopy, shifts from 80 to 500 cm^{-1} at $p=30$ GPa,[28] and the phonon frequencies, measured indirectly from IR active phonon sidebands, increases up to 900 cm^{-1} reaching a pressure of 80 GPa.[20,29] For lower pressure, we can compare with measurements performed in pure H_2 at low temperature.[17,18] The similar frequency range where these bands appear in $Ar(H_2)_2$ and in solid H_2 testify for the similar origin of these excitations, that is, phonon excitation due to the hydrogen molecules.

The nature of the various bands has been disclosed principally from their slope analysis. The parameters of the polynomial fit of the frequencies of the various bands are listed in Table II, together with values, obtained from the literature, referring to pure H_2. Remarkable are the similarities among the slopes of the different class of bands in this compound and in pure H_2. In summary, we identify three classes of slopes. For the pure roton $\Omega_1 = 1-2$ cm^{-1}/GPa, almost identical to the case of in natural solid H_2. For the pure vibron $\Omega_1 = 9-11$ cm^{-1}/GPa, which is very similar for solid H_2 if obtained from a fit in the same pressure range. For the vibron plus rotation $\Omega_1 = 13-17$ cm^{-1}/GPa (for solid H_2 this value depends on pressure, and amounts to about 9 if obtained in an analogous pressure range). For the phonon combination band $\Omega_1 = 30-40$ cm^{-1}/GPa, that compares favorably with solid H_2 if analyzed in a similar pressure range. The interpretation of these four cases is already documented in the hydrogen literature.[1,11]

V. DISCUSSION

A. Splitting of vibron at low temperature

Our low temperature spectra are displayed in Fig. 4. On cooling the sample the zero-phonon line $Q_1(J)$ splits into a doublet [see Fig. 6(a)]. Two possible causes are proposed to explain this behavior. First, the degeneracy of the infrared mode (E_{1u}) may be removed, due to a strong decrease of the crystal quality, or to a phase transition to a lower symmetry unit cell. Otherwise, the high and low frequency components of the infrared vibron are to be attributed to the $Q_1(0)$ and $Q_1(1)$ transitions of the hydrogen molecule, respectively. This splitting is not observed, for example, in the Raman scattering of compressed H_2 at room temperature because of motional narrowing,[33] but may become evident in this case, where a symmetry allowed IR vibron mode is observed at low temperature. In the IR spectrum of natural H_2 at 4.2 K, the splitting of the vibron is observed up to 1 GPa, and amounts to about 6.3 cm^{-1}.[19]

The size of the splitting increases, decreasing temperature, from 3.5 cm^{-1} at 200 K to 6 cm^{-1} at $T \simeq 35$ K, a value about that of the gas phase.[34,35] The interpretation of this behavior is unclear. It should be noted, however, that in the solid H_2 at room temperature the two Raman lines merge, while they are separated at low temperature.

If this interpretation is correct, the measured intensity of the para component $Q_1(0)$ should increase with respect to the ortho component $Q_1(1)$, cooling the sample. This is actually what we observe, the intensity ratio $Q_1(0)/Q_1(1)$ varying from 0.3, at the highest temperature where we observe this component, to 0.6 at 35 K. In addition the intensity

of the combination band $Q_1(J)+S_0(0)$ increases, and its ratio with the ortho component $Q_1(J)+S_0(1)$ grows from a value of 0.6 at 300 K to 1.0 at 35 K (see Fig. 4).

Another effect due to the ortho-para conversion is the decrease of the global intensity of the depolarized broad vibron band. As discussed in the previous section, this band is indeed induced by double transitions. As found experimentally by Gush[16] in low temperature solid H_2, we may assume that the total intensity of this band is proportional to $3c_o^2+2c_oc_p$, where c_o and c_p are the ortho- and parahydrogen molar fractions, respectively. From both spectroscopic evidences we can estimate now the concentration of para-molecules in the compound on cooling. It results, at the three lowest temperatures of this study, 147, 97, and 35 K, respectively, of about 26–29, 31–40, and 45–50 %, lower than the equilibrium values, that are 29, 40, and 90 % at the three temperatures. Consideration of the equilibration time is then important for a complete modeling of this phenomenon. Of course it would be interesting to vary pressure in this cooled compound crystal, because pressure should accelerate the ortho-para conversion appreciably, via an increase in the magnetic spin-spin interaction varying the distance between molecules.

B. Vibrational coupling

In this section we discuss the frequency difference of the IR and Raman mode. The model of vibrational coupling is applied here, as in the pure H_2 case. Moreover, a quantitative agreement is demonstrated among the value of the coupling constant G derived here with values reported in the literature.[23,31]

The measured pressure dependence of the vibron frequency Q_q in the IR is compared with the Raman one in Fig. 7. The difference $\Delta\omega=\omega_{\mathrm{IR}}-\omega_R$ for the vibron in this compound has the same sign and is of the same order of magnitude as in pure hydrogen, even if somewhat lower (e.g., at $p=30$ GPa, it is $\simeq 60$ cm^{-1} for $Ar(H_2)_2$ and $\simeq 100$ cm^{-1} for pure solid hydrogen). This difference and the turnover or softening of both vibrons (ω_R and ω_{IR}) at different pressures in pure hydrogen have been extensively discussed in the literature recently.[31,36–38]

Common to all these discussions are the basic considerations by van Kranendonk.[39] The coupling among molecular vibrations arises from the dependence of the *intermolecular* potential energy on the *intramolecular* bond lengths of the two interacting molecules. A pair potential model suffices to reproduce the results. Following van Kranendonk, the potential energy $\Phi(R_{12},r_1,r_2)$ of two interacting H_2 molecules, averaged over all orientations, at a distance R_{12} between the centers of mass, is expanded as a function of the deviations $u_i=r_i-r_e$ of the intramolecular coordinates r_1 and r_2 from their equilibrium value r_e according to

$$\begin{aligned}\Phi(R_{12},r_1,r_2)&=\Phi(R_{12},r_e,r_e)+F_1(r_1)+F_1(r_2)\\&\quad+F_2(r_1,r_2)\\&\simeq\Phi(R_{12},r_e,r_e)+F(R_{12})(u_1^2+u_2^2)\\&\quad+G(R_{12})u_1u_2.\end{aligned}\tag{1}$$

We are here interested in the term $G(R_{12})u_1u_2$, that couples the vibrational motion of all pairs of molecules in the system. The pure H_2 crystal can then be modeled as a rigid hcp lattice of one-dimensional coupled harmonic oscillators. With two molecules per unit cell, there are two vibrational normal modes, whose frequencies have been derived solving exactly the dynamical matrix, for $k=0$ and in the assumption of only nearest-neighbor coupling.[31] Since the two vibrational modes correspond to in-phase and out-of-phase motion of the two oscillators in the unit cell, these have been identified, respectively, as the Raman and the IR mode of the H_2 crystal, even though no IR active mode exists for a rigid hcp lattice of one-dimensional harmonic oscillators.

We have extended this analysis to $Ar(H_2)_2$. The interaction potential energy of the H_2 molecules in this crystal is the same [Eq. (1)]. The presence of Ar atoms does not influence the H_2-H_2 vibrational coupling. Here, there are 8 H_2 molecules in the unit cell, and the solution requires the diagonalization of a 8×8 dynamical matrix. Moreover, the distance between the H_2 molecules is not exactly known (see Sec. II), and is different for different pairs. For the moment, we leave the positions of the H_2 molecules in the unit cell as a free parameter, that will be determined in the following analysis. This kind of information is new for this crystal, and could not be extracted from the available x-ray data.

For constructing the dynamical matrix, a cutoff distance has been set for the vibrational interaction, such that each molecule interacts with its nearest neighbors only. The hexagonal unit cell of $Ar(H_2)_2$, of dimension a and c, is represented in Fig. 1, where the relevant intermolecular distances R_1, R_2, and R_3 are indicated. The expressions for these quantities as a function of the unknown parameter $\delta\equiv u-5/6$ and of $k\equiv c/a\simeq\sqrt{8/3}$, are

$$\begin{aligned}R_1&=\frac{a}{2}(1+6\delta),\\R_2&=\frac{a}{2}(1-6\delta),\\R_3&=\frac{a}{2}\left[\frac{1}{3}(1-6\delta)^2+\frac{k^2}{4}\right]^{1/2}.\end{aligned}\tag{2}$$

The more symmetric case is that for which $\delta=0$, $k=\sqrt{8/3}$, and $R_1=R_2=R_3=a/2$, but the experimental value of k at 6.2 GPa is $1.628<\sqrt{8/3}=1.633$. The problem is tractable if we assume that the functional form for $G(R)$ is a power law, that is,

$$G(R)=G_0\left(\frac{R_0}{R}\right)^n.\tag{3}$$

This should happen at low density, with $n=6$, and it has been demonstrated to hold (with $n\simeq 7$) in the density range relevant for this study.[31] We can, therefore, define three proportionality factors α_i ($i=1$, 2, or 3) that satisfy

$$G(R_i)=\alpha_iG\left(\frac{\alpha}{2}\right)\tag{4}$$

TABLE III. Frequencies and symmetries of the $k=0$ vibron modes in $Ar(H_2)_2$.

$\omega^2\mu$	$\omega^2\mu$ $\alpha_1=\alpha_2=\alpha_3=1$	Symmetry	Activity
$F+G(\alpha_1+\alpha_2)+G\sqrt{(\alpha_1+\alpha_2)^2+12\alpha_3^2}$	$F+6G$	A'_{1g}	Raman
$F-G(\alpha_1+\alpha_2)$	$F-2G$	E_{2g}	Raman
$F+2G(\alpha_1+\alpha_2)$	$F+4G$	B_{1u}	inactive
$F-G(\alpha_1+\alpha_2)$	$F-2G$	E_{1u}	IR
$F+G(\alpha_1+\alpha_2)-G\sqrt{(\alpha_1+\alpha_2)^2+12\alpha_3^2}$	$F-2G$	A''_{1g}	Raman
F	F	B_{2g}	inactive

in such a way that in all the formulas the function $G(R)$ appears for the same value of the independent variable. The proportionality factors α_i can be derived easily from Eqs. (2), (3), and (4).

The dynamical matrix can be written without difficulty, and is diagonalized with the aid of algebraic manipulation programs. The resulting eight eigenvalues determine the frequencies of the normal modes, that are listed in Table III. The symmetry of each normal mode has been derived considering the transformation properties of the eigenvectors by the application of the symmetry operations of the D_{6h}^4 space group. Note that an additional accidental degeneracy, due to the simplified interaction assumed, makes the frequencies of the E_{1u} and E_{2g} modes coincident.

The observed Raman mode is A'_{1g}, which corresponds to the in-phase vibration of all eight molecules. The other Raman active modes (E_{2g}, and A''_{1g}), whose frequency should be very close to that of the IR active mode, are not observed in this study, probably because they are very weak, since correspond, according to their eigenvector, to vibrations where pairs of molecules oscillate with opposite phases. A reliable calculation of the intensity of the Raman active mode, through the unit cell vibration polarizability, would also be possible with the knowledge of the normal mode eigenvectors, but it is beyond the scope of the present work.

From the difference between the squares of the IR and Raman frequency we calculate the quantity

$$\Delta \equiv \frac{1}{2\pi}\frac{\omega_{\mathrm{IR}}^2-\omega_R^2}{\mu} = -G[2(\alpha_1+\alpha_2)+\sqrt{(\alpha_1+\alpha_2)^2+12\alpha_3^2}]$$
$$\simeq -8G, \tag{5}$$

where μ is the reduced mass for the nuclear motion. As Δ is positive, G is negative, as in pure hydrogen. Both Δ and G are functions of the intermolecular distance or, equivalently, of the pressure. In the case of pure H_2 we have, for the same quantity $\Delta_{H_2}=-12G$. This is due to the higher number of nearest neighbors (12) in H_2 with respect to $Ar(H_2)_2$ (6), and, generally, to the different crystal structure.

The quantity $\Delta/8$, that coincides with $-G(R)$ in the hypothesis of $\delta=0$ and $k=\sqrt{8/3}$, is plotted as a function of the intermolecular distance in Fig. 10, obtained from the fitted pressure behavior of the frequency. The unit cell dimension a has been derived from the measured pressure by the experimental determined x-ray equation of state.[40] In the same figure two other determinations of $G(R)$ are reported, namely, the one by Loubeyre *et al.*[31] and by Moshary *et al.*[23] There is very good agreement among our determination in $Ar(H_2)_2$ and the data of pure H_2. The larger difference, in fact, amounts to about 12%. This testifies on the correctness of the interaction model, and confirms that we are dealing with a parameter describing fundamental interaction properties among hydrogen molecules.

Unfortunately a significantly better agreement cannot be obtained by changing the parameters δ and k, from which α_1, α_2, and α_3 depend [we assume $n=7$ in Eq. (3)]. We have mantained k fixed to the experimental value of 1.628, measured at 6.2 GPa. In this case, the difference between G_{exp} and the data of the other authors has a minimum for $\delta\simeq-0.004$. The change, however, is not significant, as shown in Fig. 10. On the other hand, if δ changes slightly from this value, G_{exp} becomes rapidly much smaller. If we accept a maximum difference of about 20% between our G_{exp} and previous values, it should be $-0.015<\delta<+0.008$. This gives for the distance between the H_2 molecules $1.048\times a/2>R_1>0.910\times a/2$, $0.952\times a/2<R_2<1.090\times a/2$.

VI. CONCLUSIONS

With pressure, solid hydrogen should present a fascinating evolution from an archetype quantum molecular solid towards the long-sought quantum metal. Unfortunately, the pressure of metallization of hydrogen is still outside the present experimental possibility. The $Ar(H_2)_2$ compound was proposed as an alternative to solid hydrogen for observing this evolution. We have shown through this infrared study that the $Ar(H_2)_2$ compound presents many of the quantum molecular properties of solid hydrogen. In particular, the systematic comparison of spectroscopic data of

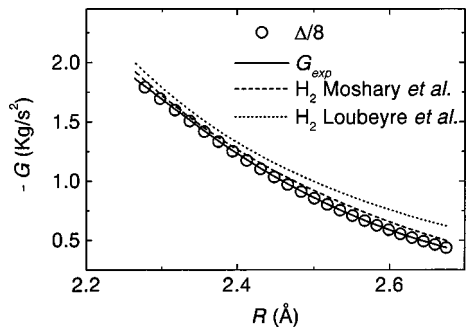

FIG. 10. Experimentally determined force constant $-G(R)$ among two hydrogen molecules, compared with analogous determination by Loubeyre *et al.* (Ref. 31) and by Moshary *et al.* (Ref. 23).

$Ar(H_2)_2$—such as frequency ω $(p \rightarrow 0)$, bandwidth Γ $(p \rightarrow 0)$, and their pressure dependence—produces evidence of quasifree rotating molecules in the compound, the existence of an unpolarized spectrum, a dependence of this spectrum on the concentration of the orthomolecules, and a vibrational coupling between H_2 molecules identical to the one of pure solid H_2. Therefore, the present data suggests that the similarity between pure H_2 and $Ar(H_2)_2$ from low pressure to Mbar pressure is more remarkable than commonly thought.

The FTIR spectra in the combination mode region of the H_2 molecule turned out to be quite complex. We achieved a full assignment of band maxima as a function of pressure and temperatures and gained insight into the excitation of hydrogen modes of all kinds such as vibron, vibron plus phonon, and vibron plus roton. In cooling the sample we were able to study in detail the ortho-para intensity ratio as well its frequency splitting. Also, a strong elastic anisotropy of the compound was observed that could explain why some controversial results between Raman and infrared studies have been obtained at very high pressures.

ACKNOWLEDGMENTS

The authors wish to thank Dr. Frederic Datchi for his help during part of this experiment. This work has been supported by the European Union under Contract No. ERB FMGE CT950017. One of us (H.J.J.) expresses his thanks to NATO (Grant No. 950285).

*Electronic address: ulivi@ieq.fi.cnr.it

[1] H. K. Mao and R. J. Hemley, Rev. Mod. Phys. **66**, 671 (1994).
[2] W. L. Vos, L. W. Finger, R. J. Hemley, J. Z. Hu, H. K. Mao, and J. A. Schouten, Nature (London) **358**, 46 (1992).
[3] P. Loubeyre, M. Jean-Louis, R. LeToullec, and L. Charon-Gérard, Phys. Rev. Lett. **70**, 178 (1993).
[4] M. S. Somayazulu, L. W. Finger, R. J. Hemley, and H. K. Mao, Science **271**, 1400 (1996).
[5] P. Loubeyre, R. Le Toullec, and J. P. Pinceaux, Phys. Rev. Lett. **72**, 1360 (1994).
[6] S. Bernard, P. Loubeyre, and G. Zerah, Europhys. Lett. **37**, 477 (1997).
[7] P. Loubeyre, R. LeToullec, D. Hausermann, M. Hanfland, R. J. Hemley, H. K. Mao, and L. W. Finger, Bull. Am. Phys. Soc. **41**, 564 (1996).
[8] J. B. Friauf, Phys. Rev. **29**, 34 (1927).
[9] T. Ohba, Y. Kitano, and Y. Komura, Acta Crystallogr., Sect. C: Cryst. Struct. Commun. **40**, 1 (1984).
[10] Y. Komura and K. Tokunaga, Acta Crystallogr., Sect. B: Struct. Crystallogr. Cryst. Chem. **36**, 1548 (1980).
[11] I. Silvera, Rev. Mod. Phys. **52**, 393 (1980).
[12] R. LeToullec, J. P. Pinceaux, and P. Loubeyre, High Press. Res. **1**, 77 (1988).
[13] H. K. Mao, P. M. Bell, J. V. Shaner, and D. J. Steinberg, J. Appl. Phys. **49**, 3276 (1978).
[14] R. Bini, L. Ulivi, H. J. Jodl, and P. R. Salvi, J. Chem. Phys. **103**, 1353 (1995).
[15] R. Bini, R. Ballerini, G. Pratesi, and H. J. Jodl, Rev. Sci. Instrum. **68**, 3154 (1997).
[16] H. P. Gush, W. F. J. Hare, E. J. Allin, and H. L. Welsh, Can. J. Phys. **36**, 177 (1960).
[17] M. Jean-Louis, Chem. Phys. Lett. **51**, 254 (1977).
[18] A. Coulon and M. Jean-Louis, in *High Pressure Science and Technology*, edited by B. Vodar and Ph. Marteau (Pergamon Press, Oxford, 1980).
[19] M. Jean-Louis and H. Vu, Rev. Phys. Appl. **7**, 89 (1972).
[20] M. Hanfland, R. J. Hemley, H. K. Mao, and G. P. Williams, Phys. Rev. Lett. **69**, 1129 (1992).
[21] V. F. Sears and J. Van Kranendonk, Can. J. Phys. **42**, 980 (1964).
[22] M. L. Klein and T. R. Koehler, in *Rare Gas Solids*, edited by M. L. Klein and J. A. Venables (Academic Press, London, 1976), p. 326.
[23] F. Moshary, N. H. Chen, and I. F. Silvera, Phys. Rev. B **48**, 12 613 (1993).
[24] R. J. Hemley, H. K. Mao, L. W. Finger, A. P. Jephycoat, R. M. Hazen, and C. S. Zha, Phys. Rev. B **42**, 6458 (1990).
[25] P. Loubeyre, R. LeToullec, D. Hausermann, M. Hanfland, R. J. Hemley, H. K. Mao, and L. W. Finger, Nature (London) **383**, 702 (1996).
[26] L. Ulivi, M. Zoppi, L. Gioè, and G. Pratesi, Phys. Rev. B **58**, 2383 (1998).
[27] A. Driessen, V. D. Poll, and I. F. Silvera, Phys. Rev. B **30**, 2517 (1984).
[28] R. J. Hemley, J. H. Eggert, and H. K. Mao, Phys. Rev. B **48**, 5779 (1993).
[29] M. Hanfland, R. J. Hemley, and H. K. Mao, in *High-Pressure Science and Technology*, edited by S. C. Schimdt, J. W. Shaner, G. A. Samara, and M. Ross (AIP, New York, 1994), p. 877.
[30] K. D. Bier, H. J. Jodl, and H. Däufer, Can. J. Phys. **66**, 708 (1988).
[31] P. Loubeyre, R. Le Toullec, and J. P. Pinceaux, Phys. Rev. B **45**, 12 844 (1992).
[32] R. J. Kriegler and H. L. Welsh, Can. J. Phys. **46**, 1181 (1968).
[33] N. E. Moulton, G. H. Watson, W. B. Daniels, and D. M. Brown, Phys. Rev. A **37**, 2475 (1988).
[34] S. Bhatnagar, E. J. Allin, and H. Welsh, Can. J. Phys. **40**, 8 (1962).
[35] J. L. Feldmann, J. H. Eggert, J. de Kinder, R. J. Hemley, H. K. Mao, and D. Shoemaker, Phys. Rev. Lett. **74**, 1379 (1995).
[36] L. Cui, N. H. Chen, and I. F. Silvera, Phys. Rev. B **51**, 14 987 (1995).
[37] I. F. Silvera, S. J. Jeon, and H. Lorenzana, Phys. Rev. B **46**, 5791 (1992).
[38] D. M. Brown and W. B. Daniels, Phys. Rev. A **45**, 6429 (1992).
[39] J. van Kranendonk, *Solid Hydrogen* (Plenum, New York, 1983).
[40] P. Loubeyre (unpublished).